

Arabidopsis COP1/SPA1 Complex and FHY1/FHY3 Associate with Distinct Phosphorylated Forms of Phytochrome A in Balancing Light Signaling

Yusuke Saijo,^{1,4} Danmeng Zhu,^{1,2} Jigang Li,¹ Vicente Rubio,^{1,5} Zhenzhen Zhou,¹ Yunping Shen,^{1,2,7} Ute Hoecker,³ Haiyang Wang,^{1,6} and Xing Wang Deng^{1,*}

¹Department of Molecular, Cellular and Developmental Biology, Yale University, New Haven, CT 06520, USA

²Peking-Yale Joint Center of Plant Molecular Genetics and Agrobiotechnology, College of Life Sciences, Peking University, Beijing 100871, People's Republic of China

³Institute of Botany, University of Cologne, D-50931 Cologne, Germany

⁴Present address: Department of Plant-Microbe Interactions, Max Planck Institute for Plant Breeding Research, D-50829 Cologne, Germany

⁵Present address: Centro Nacional de Biotecnología, Consejo Superior de Investigaciones Científicas, Madrid, 28049, Spain

⁶Present address: Boyce Thompson Institute for Plant Research, Cornell University, Ithaca, NY 14853, USA

⁷Present address: Department of Molecular, Cell, and Developmental Biology, University of California, Los Angeles, Los Angeles, CA 90095, USA

*Correspondence: xingwang.deng@yale.edu

DOI 10.1016/j.molcel.2008.08.003

SUMMARY

Fine tuning of light signaling is crucial to plant development. Following light-triggered nuclear translocation, the photoreceptor phytochrome A (phyA) regulates gene expression under continuous far-red light and is rapidly destabilized upon red light irradiation by E3 ubiquitin ligases, including COP1. Here we provide evidence that the light signaling repressors SPA proteins contribute to COP1-mediated phyA degradation and that a COP1/SPA1 protein complex is tightly associated with phyA ubiquitination activity. Furthermore, a phosphorylated phyA form accumulates in the nucleus and preferentially associates with the COP1/SPA1 complex. In contrast, underphosphorylated phyA predominantly associates with the phyA-signaling intermediates FHY3 and FHY1. However, COP1 associates with underphosphorylated phyA in the absence of FHY3 or FHY1, suggesting that phyA associations with FHY3 and FHY1 protect underphosphorylated phyA from being recognized by the COP1/SPA complex. We propose that light-induced phyA phosphorylation acts as a switch controlling differential interactions of the photoreceptor with signal propagation or attenuation machineries.

INTRODUCTION

Plants monitor light by a set of photoreceptors such as phytochromes (phys) to optimize development. Phys are dimeric chromoproteins that undergo photoconversion between the red light (600–700 nm; R) absorbing Pr form and the far-red light (700–750 nm; FR) absorbing, biologically active Pfr form (Chen et al., 2004). Light activation of phys induces their nuclear translocation (Nagatani, 2004; Nagy and Schafer, 2002), thereby reprogram-

ming gene expression through direct interaction with several transcription factors of the bHLH family, including PIF3 and PIF3-like proteins (Al-Sady et al., 2006; Bauer et al., 2004; Hiltbrunner et al., 2005; Khanna et al., 2004; Martinez-Garcia et al., 2000). In *Arabidopsis*, phyA is the primary photoreceptor for responses to continuous far-red light (FRc), termed FR high irradiance response (FR-HIR), and is rapidly degraded upon exposure to red or white light (Chen et al., 2004; Clough and Vierstra, 1997). Genetic and genomic evidence points to a pivotal role of two sets of nuclear factors in phyA signaling: FHY1 and FHL that promote phyA nuclear accumulation (Desnos et al., 2001; Zhou et al., 2005) and FHY3 and FAR1 that act as transcription factors essential for *FHY1/FHL* gene expression (Hudson et al., 1999; Lin et al., 2007; Wang and Deng, 2002; Wang et al., 2002). These findings indicate that critical phyA signaling events occur within the nucleus (Chen et al., 2004; Nagatani, 2004; Nagy and Schafer, 2002).

In the R-induced phyA destabilization, the photomorphogenic repressor protein COP1 acts as an E3 ubiquitin ligase that directly binds and targets phyA for degradation (Seo et al., 2004). COP1 also targets several photomorphogenesis-promoting transcription factors for degradation (Jang et al., 2005; Osterlund et al., 2000; Saijo et al., 2003; Seo et al., 2003, 2004; Yang et al., 2005). COP1 contains a RING-finger domain, a coiled-coil domain, and a WD40 domain that directly recognizes its substrate proteins (Holm et al., 2001). COP1 is present as part of large protein complex(es) that also contains the nuclear-resided light signaling repressor SPA1 (Hoecker et al., 1999; Saijo et al., 2003). SPA1 is a member of the WD40 domain-containing SPA protein family and was shown to modulate the E3 ligase activity of COP1 in vitro (Saijo et al., 2003; Seo et al., 2003). Genetic and biochemical data suggest that all four SPA proteins (SPA1–SPA4) work together with COP1 in repressing light signaling (Hoecker, 2005; Laubinger et al., 2004). However, the precise mechanisms by which SPA proteins support COP1-mediated substrate ubiquitination remain unclear.

Reversible phosphorylation has also been described as a signal-attenuating mechanism for phyA: phosphorylated phyA

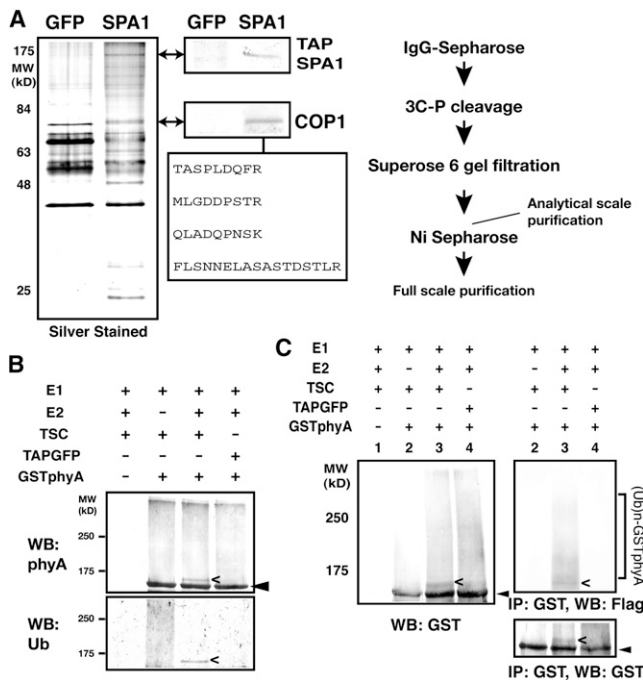


Figure 1. The COP1/SPA1 Complex Associates with an E3 Activity for phyA Ubiquitination

(A) TAPSPA1 copurified proteins from seedlings following the purification scheme (right) were resolved by SDS-polyacrylamide gel electrophoresis (SDS-PAGE) and silver-stained. Immunoblots with anti-myc (for TAPSPA1) and anti-COP1 antibodies are presented (middle). The box shows COP1 peptide fragments identified by mass spectrometry analysis. GFP, TAPGFP; SPA1, TAPSPA1; IgG, Immunoglobulin G; 3C-P, 3C protease. (B and C) phyA ubiquitination by TSC in vitro. Purified TSC (B) and an analytical scale TSC fraction (C), as well as their corresponding TAPGFP controls, were assayed for E3 activity on GSTphyA. Ubiquitinated products were detected by immunoblotting (WB) with anti-phyA and ubiquitin (Ub) antibodies (B) or with anti-phyA and Flag antibodies (C). phyA was recovered by immunoprecipitation (IP) with anti-GST antibodies (C). The open and closed arrowheads indicate positions of apparently monoubiquitinated and unmodified phyA, respectively.

shows low Pfr stability in vivo and low affinity in vitro for signaling intermediates (Kim et al., 2004; Ryu et al., 2005). Previous studies have identified phosphorylation sites on oat phyA (Lapko et al., 1999; Yeh and Lagarias, 1998), of which distinct phosphorylation sites seem to affect the stability and protein-protein interactions of the photoreceptor (Kim et al., 2004; Ryu et al., 2005). However, it remains to be elucidated how phyA phosphorylation status is linked to signal propagation or attenuation in vivo. Our data suggest that phosphorylation-dependent sorting of phyA into different protein complexes provides a molecular basis for balanced control of plant development in changing light environment.

RESULTS AND DISCUSSION

In an attempt to purify the presumed COP1-SPA1 complex(es), we employed a modified tandem affinity purification (TAP)-based procedure (Saijo et al., 2003) to isolate SPA1-associated proteins in *Arabidopsis* (Figure 1A). As expected, both COP1 and

SPA1 proteins copurified throughout the TAP procedure (Figure 1A). Gel filtration analysis confirmed cofractionation of both proteins in the purified samples (Figure S1 available online). Mass spectrometry analysis of an ~72 kDa band specifically associated with TAPSPA1 showed a 100% match to COP1 (Figure 1A). In contrast, phyA was not copurified throughout the TAP procedure, indicating that phyA is not an integral component of the COP1/SPA1 complex(es) (Figure S1B), despite evident coprecipitation of TAPSPA1 with phyA (Figure S1C).

We then examined the E3 activity of isolated TAPSPA1 and COP1 complex (TSC) toward phyA in vitro, using recombinant *Arabidopsis* phyA fused with glutathione S-transferase (GSTphyA) as the substrate. Neither the photoconversion nor absence of the chromophore influenced in vitro phyA ubiquitination by recombinant COP1 (Seo et al., 2004). We detected a size shift consistent with monoubiquitination of phyA when incubated with TSC sample, but not with the TAPGFP control, in the presence of recombinant E1 and E2 (Figure 1B). At present, the biological significance of phyA monoubiquitination is unknown. We further tested whether the COP1/SPA1 complex mediates phyA polyubiquitination that generally leads to subsequent proteasomal degradation (Jabben et al., 1989; Pickart, 2001). To facilitate specific detection of ubiquitinated phyA, we developed a procedure using Flag-tagged ubiquitin (Ub) and partially purified TSC at an analytical scale. We recovered GSTphyA from the E3 assay reactions and then performed immunoblot analysis with anti-Flag antibody. We detected the attachment of Flag-Ub to GSTphyA in both high molecular weight (polyubiquitinated) as well as apparent monoubiquitinated GSTphyA forms, specifically when incubated with the TSC sample (Figure 1C). Copurification and, hence, tight association of the COP1/SPA1 complex with robust E3 activity for phyA supports a notion that the COP1/SPA1 complex(es) represents the core biochemical entity of an E3 ligase responsible for phyA ubiquitination.

We next characterized the endogenous COP1/SPA1 complex. SPA1 abundance is elevated under FRc in the wild-type, but not in a *phyA-101* null mutant, indicating that phyA is responsible for the increase in SPA1 accumulation under FRc (Figure 2A). As previously reported (Fittinghoff et al., 2006), SPA1 is more abundant under various light conditions compared to darkness (Figure 2B). We then verified endogenous COP1-SPA1 interaction by coimmunoprecipitation (co-IP) analysis of the two proteins (Figure 2A). Although essentially the same amounts of COP1 were precipitated with COP1-specific antibodies, the yield of SPA1 in COP1 co-IP was slightly higher under all light conditions examined than under darkness (Figures 2A and 2B), likely reflecting the elevation in total SPA1 abundance under light conditions. A phyA-induced SPA1 accumulation followed by enhanced COP1-SPA1 association may serve to desensitize phyA-signaling under FRc. In addition, the results support the previous finding that SPA1 also functions under light conditions other than FRc (Fittinghoff et al., 2006). Moreover, SPA1 accumulates to higher levels in the hyperphotomorphogenic *cop1* mutant backgrounds than in a wild-type background (Figure 2C). Furthermore, gel filtration analysis of endogenous COP1 and SPA1 showed their cofractionation (Figure 2D). The size of endogenous SPA1 peak fractions (Fractions 8–10 in Figure 2D) was essentially the same as that of purified TSC (Figure S1A).

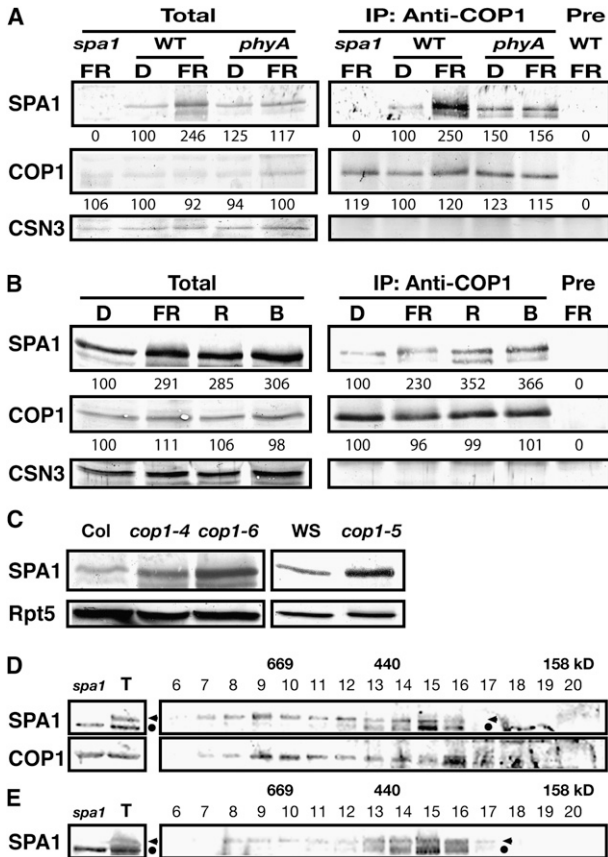


Figure 2. Endogenous COP1/SPA1 Complex Characterization
 (A) phyA-induced SPA1 accumulation and SPA1-COP1 interaction. COP1 coimmunoprecipitates were analyzed by immunoblotting with the indicated antibodies on the left. Pre, control immunoprecipitation (IP) with the preimmune sera. D, continuous darkness; FR, continuous far-red light. All genotypes used are in the RLD background.
 (B) SPA1 co-IP of SPA1 from the wild-type RLD under various light conditions. R, continuous red light; B, continuous blue light. Numbers under lanes in (A) and (B) indicate relative band intensities that were quantified and normalized for each panel.
 (C) Immunoblotting of dark-grown seedling lysates. CSN3 (A and B), and Rpt5 (C) were monitored as loading controls. WS, the Wassilewskija ecotype.
 (D and E) Gel filtration profiles of SPA1 and COP1 in the dark-grown wild-type RLD (D) and a *cop1-5* null mutant (E). T and *spa1* represent total lysate inputs and those from *spa1-3* used for gel filtration, respectively. The fraction numbers and molecular weight are indicated above. The arrowhead and dot indicate SPA1 and a crossreacting band recognized by anti-SPA1 antibodies, respectively.

However, the SPA1 peak fractions were slightly shifted toward smaller size in the *cop1-5* null mutant (Figure 2E), supporting the idea that SPA1 acts as part of the COP1 complex(es).

To examine functional significance of the COP1/SPA1 protein complex in phyA degradation, we monitored phyA degradation kinetics in the *spa1 spa2 spa3* and *spa1 spa2 spa4* triple mutants, considering genetic redundancy among the SPA genes (Laubinger et al., 2004). Both *spa* triple mutants exhibited a delay in Rc-induced phyA degradation similar to *cop1-4* (Figure 3A). Thus, SPA proteins indeed contribute to phyA degradation. All

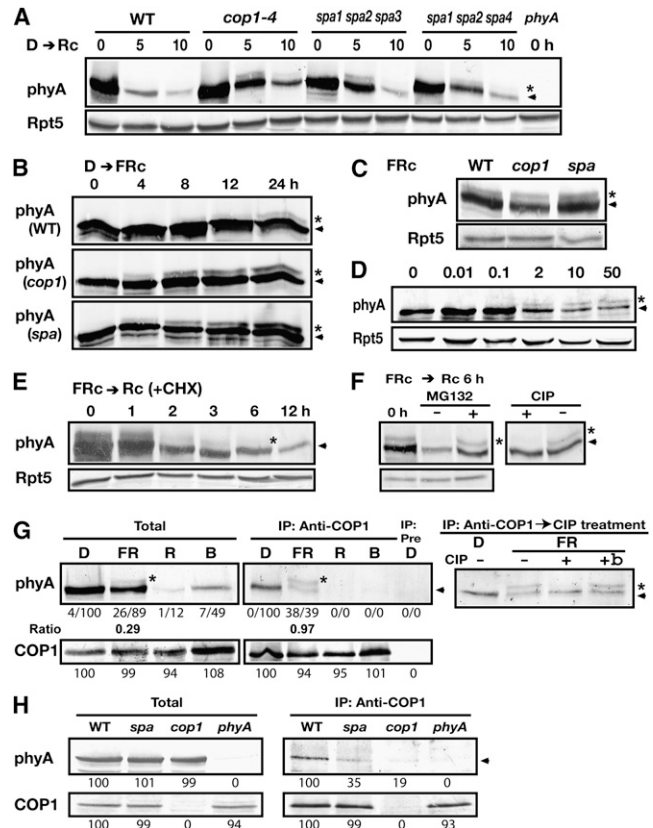


Figure 3. The COP1/SPA Complex(es) Preferentially Associate with Phosphorylated phyA In Vivo

(A and B) Five-day-old dark-grown seedlings exposed to Rc (A) or FRC (B) for the indicated times and FRC-grown seedlings (C and D) were subjected to immunoblot analyses. The *cop1-4* (*cop1*), *spa1spa2spa3* (*spa*), *spa1spa2spa4*, *phyA-201* (*phyA*) mutants, and wild-type (WT) were used. Rpt5 was monitored as a loading control in (A) and (C)–(F). The numbers above the panel indicate FRC fluence rate ($\mu\text{mol}/\text{m}^2/\text{s}$) in (D). The asterisk and arrowhead represent positions of the large and unmodified phyA forms in (A)–(E), respectively. (E) Immunoblot analysis of FRC-grown seedlings exposed to Rc for the indicated times in the presence of 100 μM cycloheximide. (F) FRC-grown seedlings pretreated with or without 50 μM MG132 were transferred to Rc for 6 hr. Lysates of the MG132-treated plants were incubated with or without calf intestinal alkaline phosphatase (CIP). The asterisk and arrowhead represent the phosphorylated and underphosphorylated phyA forms, respectively, in (F)–(H). (G) Five-day-old seedlings were subjected to COP1 co-IP analysis under the indicated continuous light conditions (D, darkness; FR, far-red light; R, red light; B, blue light). Pre represents a mock IP control with the preimmune sera. Coimmunoprecipitated phyA with COP1 was incubated with CIP (+), boiled inactive CIP (+b), or without CIP (–). (H) COP1-phyA co-IP was reduced in the *cop1-4* and *spa* triple mutant under darkness. Numbers below immunoblots indicate relative band intensities normalized for each panel. The ratio of the phosphorylated to underphosphorylated form is shown for phyA.

SPA proteins may act as part of the COP1 E3 complex(es), as demonstrated herein with the COP1/SPA1 complex. The contribution of each SPA protein may be different, as the *spa1 spa2 spa3* mutant shows a more severe *cop1-4* mutant-like phenotype than the *spa1 spa2 spa4* mutant in phyA-dependent responses (Figure S2; Laubinger et al., 2004). However, it is notable that light-induced phyA degradation still occurs in the null

cop1-5 allele, revealing the presence of a COP1-independent phyA-degradation pathway (Figure S3A). Interestingly, no significant defect was observed for pulsed R-induced phyA degradation in the *cop1* mutants tested (Figure S3B), suggesting that the COP1-dependent and -independent pathways contribute differentially to the light-induced phyA elimination under distinct light conditions.

We noticed that a slow-migrating (or large) phyA form accumulates in the *cop1* and *spa* triple mutants upon continuous R (Rc), but not in the wild-type (Figure 3A). The large phyA band was not detectable in darkness despite high phyA abundance (Figure 3A) as well as during pulsed R-induced degradation (Figure S3B). It was reported that low rate of phyA degradation occurs upon FRc (Clough and Vierstra, 1997). We found that a large phyA form accumulates when dark-grown seedlings were exposed to prolonged FRc (for approximately 8 hr in the wild-type, Figure 3B). Noticeably, the large phyA form emerges significantly earlier and is more abundant at early time points (4–8 hr) in the *cop1* and *spa* triple mutants than in the wild-type (Figure 3B). We were unable to detect this phyA form in 2–60 min upon Rc or FRc (data not shown), a time period during which a phyA-GFP fusion is relocalized to the early-type nuclear speckles (Baer et al., 2004). These data suggest that both prolonged Rc and FRc facilitate the large phyA formation and that this modified phyA form may be a preferred target for COP1-mediated degradation. However, COP1 and SPA proteins seem to have little effect on the overall phyA steady-state levels under extended FRc (5 days), as no marked differences in phyA levels were observed among the wild-type, *cop1*, and *spa* triple mutants (Figure 3C). In addition, we observed that high fluence rates of FRc promote the formation of the large phyA species (Figure 3D).

We then examined whether both phyA forms are destabilized upon Rc. When transferring FRc-grown seedlings to Rc in the presence of the protein synthesis inhibitor cycloheximide, the amount of both phyA forms declines rapidly (Figure 3E). Pretreatment of plants with the proteasome inhibitor MG132 stabilized both phyA forms (Figure 3F). Subsequent incubation with protein phosphatase specifically diminished the large phyA form (Figure 3F). Thus, we conclude that the large and small phyA forms represent phosphorylated and underphosphorylated phyA, respectively. The results also suggest that Rc-induced elimination of both phyA forms is dependent on the 26S proteasome pathway.

To determine which form of phyA might be the preferred substrate for COP1-mediated degradation, we performed co-IP analysis for endogenous proteins (Figure 3G). Interestingly, the large phyA band was significantly enriched through the co-IP with COP1 under FRc, compared to the underphosphorylated phyA form (Figure 3G). Subsequent protein phosphatase treatment confirmed that the enriched large phyA form by COP1 co-IP procedure is phosphorylated phyA (Figure 3G). This suggests that COP1 preferentially associates with the phosphorylated phyA form, hereafter designated COP1-associated phosphorylated phyA (cap-phyA), under FRc. Both cap-phyA and underphosphorylated phyA are expected to be predominantly in the Pr state under FRc, with a pool of phyA photocycling between Pfr and Pr forms (Mancinelli, 1994; Shinomura et al., 2000). It is unclear whether the two photochemical forms differ

in the relevant phosphorylation status. Given the requirement of prolonged exposure to FRc at a high fluence rate for cap-phyA accumulation (Figures 3B and 3D and Figure S3C), cap-phyA-mediated modulation of phyA signaling may be more pronounced under prolonged than pulsed FR. In dark-grown seedlings, COP1 co-IP recovers only underphosphorylated phyA, consistent with the lack of cap-phyA detection from total protein extracts (Figure 3G). We were unable to observe robust co-IP between COP1 and cap-phyA upon a brief Rc treatment of dark-grown seedlings, when active phyA ubiquitination and its immediate degradation are expected to occur.

To test whether SPA proteins help COP1 to bind phyA, we compared COP1-phyA association between the *spa1 spa2 spa3* triple mutant and wild-type plants. To facilitate the comparison, we performed co-IP analysis with dark-grown seedlings from which high amount of phyA is readily recovered in COP1 co-IP (Figure 3G). phyA levels are essentially the same in the wild-type as in the *spa* triple mutant (Figure 3H). However, the yield of phyA in COP1 co-IP was reduced in *spa* triple mutant compared to the wild-type, whereas similar amounts of COP1 were recovered (Figure 3H). Thus, this difference may reflect a decrease in the amount of phyA associated with COP1 in the absence of 3 out of 4 SPA proteins. Our data suggest that SPA proteins likely contribute to the COP1 E3-substrate recognition, a critical step in ubiquitination (Pickart, 2001). Furthermore, SPA1 co-IP analysis indicates that SPA1-phyA association is dependent on COP1 (Figure S4). Together, our data suggest that functional COP1/SPA complex(es) may be required for effective recognition of phyA.

In light of the notion that the majority of COP1/SPA proteins and phyA is distributed in different subcellular compartments (nuclear and cytosolic, respectively) under darkness, we suspected a possibility that their interaction might occur during our IP procedure. To localize both phyA forms, we performed biochemical fractionation of the endogenous proteins from the wild-type seedlings. COP1 and phyA were detected in the nuclear fraction under all light conditions tested. Notably, we also detected a low level of phyA in the nuclear fraction of dark-grown seedlings (Figure 4A). phyA nuclear translocation is known to be mediated by both the very low fluence response and HIR. Thus, the phyA pool detected in the nuclear fraction of dark-grown seedlings was likely generated by brief exposure to white light before seedling germination in our procedure. Strikingly, cap-phyA was found to accumulate at high levels in the nucleus of FRc-grown seedlings, but not of seedlings exposed to red light.

We next explored potential phyA interactions with the nuclear-localized phyA-signaling intermediates FHY3 and FHY1. Anti-FHY3 antibodies detected endogenous FHY3 in the nuclear fraction (Figure 4A). Co-IP with anti-FHY3 antibodies using FRc-grown seedlings predominantly recovered underphosphorylated phyA (Figure 4B, IP1). Similar results were obtained with anti-FHY1 co-IP (Figure 4B, IP2). By contrast, there is an enrichment of cap-phyA in SPA1 co-IP (Figure 4B, IP3, and Figure S4), reminiscent of COP1 co-IP results (Figure 3G). Thus, it appears that underphosphorylated phyA predominantly associates with FHY3 and FHY1, through which phyA signaling may occur. However, the exact molecular mechanisms are currently unknown. On the other hand, cap-phyA seems to preferentially associate with the COP1/SPA complex(es) under FRc.

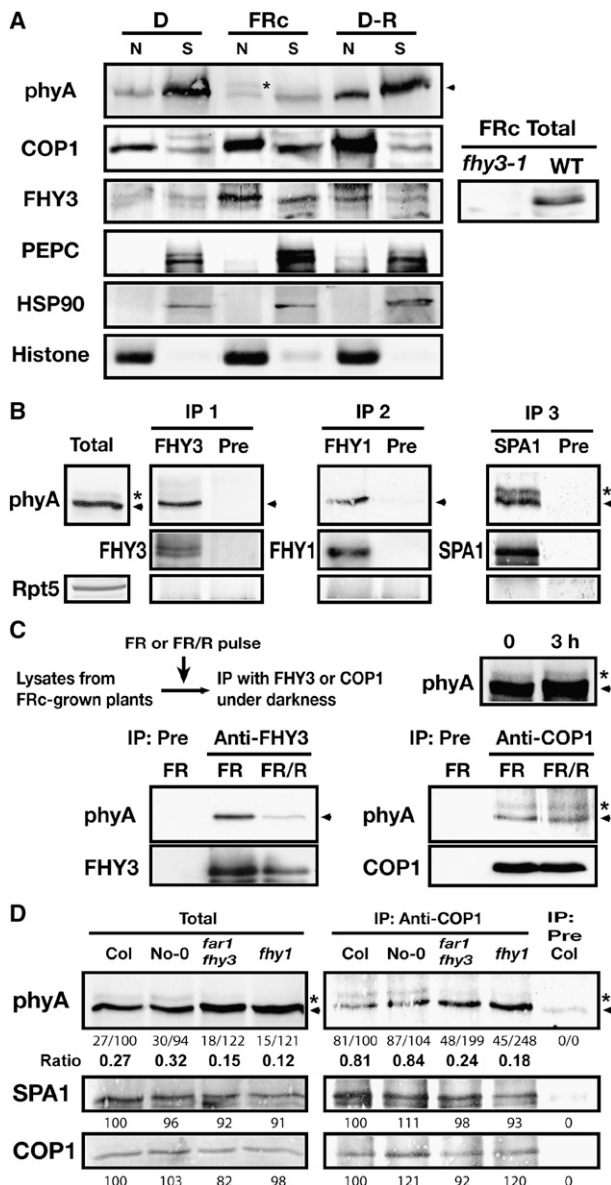


Figure 4. The Nuclear-Resident phyA-Signaling Intermediates FHY3 and FHY1 Preferentially Associate with Underphosphorylated phyA In Vivo

(A) Immunoblot analysis of purified nuclear (N) and nuclei-depleted soluble (S) fractions from 5-day-old wild-type seedlings grown under the indicated light conditions: D, continuous darkness; FR, FRC; D-R, D followed by Rc for 10 min. An approximately 12-fold quantity (in protein content) of the nuclear fraction compared to the nuclear-depleted fraction on a per-tissue-amount basis was loaded. Fraction markers used were histone H3 (Histone), cytosolic HSP90, and phosphoenolpyruvate carboxylase (PEPC). Specificity of anti-FHY3 antibodies was verified (right).

(B) Co-IP of phyA with the indicated antibodies using FRC-grown seedlings. Respective preimmune serum was used as an IP control (Pre). The Rpt5 immunoblots are shown to verify co-IP specificity.

(C) R-induced phyA-FHY3 dissociation. Design of experiments (top left): Total protein lysates of the FRC-grown phyA-overexpressing seedlings were irradiated with 5 min of FR light pulse (FR) or 5 min of FR light pulse immediately followed by 5 min of R light pulse (FR/R) and then subjected to co-IP analysis with

Under FRC, 97% of phyA is present in the Pr state at the steady-state level (Mancinelli, 1994). It has been proposed that a short-lived signal constantly generated by photocycling of phyA between the Pr and Pfr forms mediates FR-HIR (Shinomura et al., 2000). To examine the photoconversion effect on phyA associations with FHY3 and COP1, we exposed protein extracts from FRC-grown seedlings to FR or FR/R pulses before co-IP analysis. Total phyA abundance and the ratio of both phyA forms remained essentially the same during the procedure (Figure 4C). The yield of phyA in FHY3 co-IP was high with FR irradiation but greatly reduced by an R pulse following FR (Figure 4C), suggesting that the endogenous FHY3 associates more stably with Pr-phyA. If FHY3-phyA association supports signal propagation, then their R-induced dissociation is in accordance with the FR/R (but not R/FR) photoreversibility in the FR-HIR (Shinomura et al., 2000). In contrast, COP1-phyA co-IP was not significantly altered by the R/FR pulse exposure (Figure 4C).

We further examined a potential role of FHY3/FAR1 and FHY1 in the COP1-phyA interaction. We noticed that the ratio of cap-phyA versus underphosphorylated phyA is reduced in total protein extracts from both *fhy3 far1* and *fhy1* mutants (Figure 4D). The ratio of cap- versus underphosphorylated phyA in COP1 coimmunoprecipitates largely reflects that in total protein extracts from these mutants (Figure 4D). Nuclear fractionation data suggest that phyA, in particular cap-phyA, is reduced in the nucleus in these mutants (Figure S5). Therefore, FHY3/FAR1 and FHY1 may promote cap-phyA accumulation within the nucleus under FRC, which possibly serves to desensitize light-activated phyA. Strikingly, COP1 associates with high amounts of underphosphorylated phyA in the absence of either FHY3/FAR1 or FHY1. In contrast, there is no discernable alteration in COP1-SPA1 co-IP by these mutations (Figure 4D). These data imply that COP1 may not be intrinsically selective in the recognition of the distinctly phosphorylated phyA forms but bind phyA pools that are not associated with signaling intermediates. Thus, phyA-signaling intermediates such as FHY3 and FHY1 may sequester and prevent underphosphorylated phyA from associating with the COP1-SPA complex(es) under FRC.

It is unknown how many phosphorylation sites (target amino acid residues) contribute to produce cap-phyA. It could be on one or a combination of multiple sites. On oat phyA, it was reported that light-dependent Ser598 phosphorylation affects phyA interactions with signaling intermediates and that Ser7 phosphorylation influences phyA protein stability (Kim et al., 2004; Lapko et al., 1999). However, sequence alignment analysis did not reveal obvious corresponding phosphorylation residues between *Arabidopsis* and oat phyA (Figure S6). We also failed to detect a mobility shift on oat phyA expressed in *Arabidopsis* seedlings under FRC (Figure S7). Thus, it is possible that other as yet unidentified residues are involved in the generation of cap-phyA in *Arabidopsis*.

anti-FHY3 and anti-COP1 antibodies (bottom). Immunoblot analysis of lysates of FRC-grown seedlings kept under Rc for 3 hr ensured phyA stability during the procedure (top right).

(D) COP1 co-IP analysis of FRC-grown seedlings, including wild-types (Col-0 and No-0), *fhy3-1 far1-2*, and *fhy1-1*. Relative band intensities normalized for each panel and the ratio of cap-phyA to underphosphorylated phyA are shown. The asterisk and arrowhead indicate cap-phyA and underphosphorylated phyA, respectively.

Our findings support a model in which FHY3/FAR1 and FHY1 contribute to keep underphosphorylated phyA bound in a plausible signaling complex(es), limiting its vulnerability to COP1/SPA complex(es)-mediated proteolysis under FRc. Selective recruitment of underphosphorylated phyA into associations with signaling intermediates, such as FHY3 and FHY1 (Figure 4B), may lead to signal propagation. As a result, COP1 access to underphosphorylated phyA is blocked. In response to prolonged FR, a pool of cap-phyA accumulates within the nucleus and dissociates from the presumed signaling complex(es). This phyA pool is available for recognition by COP1/SPA complex(es). Thus, together with phyA-induced SPA1 accumulation (Figure 2A), phyA phosphorylation represents a feedback control to desensitize phyA signaling under FRc (Figure S8). It remains to be elucidated whether phyA-COP1 interaction plays another role beyond phyA degradation. It is also possible that cap-phyA, rather, acts as a decoy to trap the COP1/SPA complex(es) with this phyA form, thereby protecting underphosphorylated phyA. Accordingly, loss of FHY3/FAR1 or FHY1 may no longer be able to maintain the proposed phyA-signaling complex(es) in the nucleus and, thus, allows access of COP1/SPA complex(es) to underphosphorylated phyA. This model is consistent with the enrichment of cap-phyA in co-IP with COP1 and SPA1 under FRc (Figures 3G and 4B).

The lack of a detectable change in total phyA abundance in the *cop1* and *spa* triple mutants under FRc (Figure 3C) suggests that phyA recruitment into the COP1/SPA complex(es) is not sufficient to activate phyA ubiquitination and degradation. We suggest that the Pfr state of phyA may stimulate phyA ubiquitination/degradation in vivo. Under R or white light, the majority (~88%) of phyA photoconverts to the Pfr state, while under FRc, only 3% of phyA is in the Pfr state (Mancinelli, 1994). This drastic difference (about 30-fold) in the Pfr-phyA abundance under distinct light conditions might explain the vastly different rates of phyA proteolysis. Upon R-induced phyA photoconversion from the Pr to Pfr form, its interaction with COP1/SPA complex may lead to rapid ubiquitination/degradation of phyA. Furthermore, Pfr-phyA dissociation from FHY3 (Figure 4C) and light-induced FHY1 destabilization (Shen et al., 2005) should facilitate targeting of underphosphorylated phyA for degradation. Alternatively, but not mutually exclusively, Pfr-phyA may transiently act as an active signaling form prior to its degradation, as proposed with a role in PIF3 phosphorylation (Al-Sady et al., 2006). In this scenario, phyA associations with FHY3 and FHY1 may support the supply of this active phyA form. In both models, phyA dissociation from its downstream signaling components presumably accelerates phyA recruitment, regardless of its phosphorylation state, to both COP1-dependent and -independent degradation pathways (Figure S8).

EXPERIMENTAL PROCEDURES

Plant Material

Seed sterilization and plant growth were performed as previously described (Saijo et al., 2003). Detailed description of plant materials is provided in the Supplemental Data.

Protein Biochemical Experiments

Immunoblot, IP, and gel filtration analyses were performed essentially as previously described (Saijo et al., 2003). Further detailed procedures are de-

scribed in the Supplemental Data. All IP experiments in Figure 4 were performed under dim green safe light unless otherwise stated. Quantification of immunoblots was carried out with ImageJ (<http://rsb.info.nih.gov/ij/>). Band intensities of total lysates and IP samples were respectively normalized with the value of background regions and that of corresponding regions for mock IP control. Relative band intensities were then calculated for each immunoblot panel. All IP and immunoblot experiments were repeated at least three times, essentially with the same conclusions, and representative results are shown.

Purification of TSC

We introduced a functional TAPSPA1 construct (Saijo et al., 2003) into a COP1 overexpression background (McNellis et al., 1994). Five-day-old dark- or continuous white light-grown seedlings (approximately 500 g fresh weight for mass spectrometry and 20 g for an E3 assay sample) were used for the TAP procedures as described previously (Saijo et al., 2003) with the modifications described in the Supplemental Data.

In Vitro E3 Assays

The N terminal GST-tagged fusion protein with *Arabidopsis* phyA was expressed in *E. Coli* and purified using a glutathione matrix (Amersham). In vitro E3 assays were performed essentially as described previously (Saijo et al., 2003; Yang et al., 2005). Further details are provided in the Supplemental Data.

SUPPLEMENTAL DATA

The Supplemental Data include Supplemental Experimental Procedures, Supplemental References, and eight figures and can be found with this article online at <http://www.molecule.org/cgi/content/full/31/4/607/DC1/>.

ACKNOWLEDGMENTS

We thank P.H. Quail, P.S. Song, and K. Sakaguchi for providing anti-phyA antibody, *Arabidopsis* lines expressing oat phyA, and E2, respectively; J.A. Sullivan, W. Gong and O.-S. Lau for assisting with in vitro E3 assays; and V.J. Karplus for proof reading this manuscript. Our work was supported by a grant from the National Institutes of Health (GM47850) to X.W.D. Y.S. was a Japanese Society for Promotion of Science Postdoctoral Fellow, and V.R. was a Human Frontier Science Program Organization Postdoctoral Fellow.

Received: April 6, 2007

Revised: May 26, 2008

Accepted: August 4, 2008

Published: August 21, 2008

REFERENCES

- Al-Sady, B., Ni, W.M., Kircher, S., Schafer, E., and Quail, P.H. (2006). Photoactivated phytochrome induces rapid PIF3 phosphorylation prior to proteasome-mediated degradation. *Mol. Cell* 23, 439–446.
- Bauer, D., Viczian, A., Kircher, S., Nobis, T., Nitschke, R., Kunkel, T., Panigrahi, K.C.S., Adam, E., Fejes, E., Schafer, E., and Nagy, F. (2004). Constitutive photomorphogenesis 1 and multiple photoreceptors control degradation of phytochrome interacting factor 3, a transcription factor required for light signaling in *Arabidopsis*. *Plant Cell* 16, 1433–1445.
- Chen, M., Chory, J., and Fankhauser, C. (2004). Light signal transduction in higher plants. *Annu. Rev. Genet.* 38, 87–117.
- Clough, R.C., and Vierstra, R.D. (1997). Phytochrome degradation. *Plant Cell Environ.* 20, 713–721.
- Desnos, T., Puente, P., Whitelam, G.C., and Harberd, N.P. (2001). FHY1: a phytochrome A-specific signal transducer. *Genes Dev.* 15, 2980–2990.
- Fittinghoff, K., Laubinger, S., Nixdorf, M., Fackendahl, P., Baumgardt, R.L., Batschauer, A., and Hoecker, U. (2006). Functional and expression analysis of *Arabidopsis* SPA genes during seedling photomorphogenesis and adult growth. *Plant J.* 47, 577–590.

- Hiltbrunner, A., Viczian, A., Bury, E., Tscheuschler, A., Kircher, S., Toth, R., Honsberger, A., Nagy, F., Fankhauser, C., and Schafer, E. (2005). Nuclear accumulation of the phytochrome A photoreceptor requires FHY1. *Curr. Biol.* *15*, 2125–2130.
- Hoecker, U. (2005). Regulated proteolysis in light signaling. *Curr. Opin. Plant Biol.* *8*, 469–476.
- Hoecker, U., Tepperman, J.M., and Quail, P.H. (1999). SPA1, a WD-repeat protein specific to phytochrome A signal transduction. *Science* *284*, 496–499.
- Holm, M., Hardtke, C.S., Gaudet, R., and Deng, X.W. (2001). Identification of a structural motif that confers specific interaction with the WD40 repeat domain of Arabidopsis COP1. *EMBO J.* *20*, 118–127.
- Hudson, M., Ringli, C., Boylan, M.T., and Quail, P.H. (1999). The *FAR1* locus encodes a novel nuclear protein specific to phytochrome A signaling. *Genes Dev.* *13*, 2017–2027.
- Jabben, M., Shanklin, J., and Vierstra, R.D. (1989). Ubiquitin-phytochrome conjugates - pool dynamics during in vivo phytochrome degradation. *J. Biol. Chem.* *264*, 4998–5005.
- Jang, I.C., Yang, J.Y., Seo, H.S., and Chua, N.H. (2005). HFR1 is targeted by COP1 E3 ligase for post-translational proteolysis during phytochrome A signaling. *Genes Dev.* *19*, 593–602.
- Khanna, R., Huq, E., Kikis, E.A., Al-Sady, B., Lanzatella, C., and Quail, P.H. (2004). A novel molecular recognition motif necessary for targeting photoactivated phytochrome signaling to specific basic helix-loop-helix transcription factors. *Plant Cell* *16*, 3033–3044.
- Kim, J., Shen, Y., Han, Y.J., Park, J.E., Kirchenbauer, D., Soh, M.S., Nagy, F., Schafer, E., and Song, P.S. (2004). Phytochrome phosphorylation modulates light signaling by influencing the protein-protein interaction. *Plant Cell* *16*, 2629–2640.
- Lapko, V.N., Jiang, X.-Y., Smith, D.L., and Song, P.S. (1999). Mass spectrometric characterization of oat phytochrome A: Isoforms and posttranslational modifications. *Protein Sci.* *8*, 1032–1044.
- Laubinger, S., Fittinghoff, K., and Hoecker, U. (2004). The SPA quartet: A family of WD-repeat proteins with a central role in suppression of photomorphogenesis in Arabidopsis. *Plant Cell* *16*, 2293–2306.
- Lin, R., Ding, L., Casola, C., Ripoll, D.R., Feschotte, C., and Wang, H. (2007). Transposase-derived transcription factors regulate light signaling in Arabidopsis. *Science* *318*, 1302–1305.
- Mancinelli, A.L. (1994). The physiology of phytochrome action. In *Photomorphogenesis in Plants*, 2nd Edition, R.E. Kendrick and G.H.M. Kronenberg, eds. (The Netherlands: Kluwer Academic Publishers), pp. 211–269.
- Martinez-Garcia, J.F., Huq, E., and Quail, P.H. (2000). Direct targeting of light signals to a promoter element-bound transcription factor. *Science* *288*, 859–863.
- McNellis, T.W., von Arnim, A.G., and Deng, X.W. (1994). Overexpression of Arabidopsis COP1 results in partial suppression of light-mediated development - evidence for a light-inactivable repressor of photomorphogenesis. *Plant Cell* *6*, 1391–1400.
- Nagatani, A. (2004). Light-regulated nuclear localization of phytochromes. *Curr. Opin. Plant Biol.* *7*, 708–711.
- Nagy, F., and Schafer, E. (2002). Phytochromes control photomorphogenesis by differentially regulated, interacting signaling pathways in higher plants. *Annu. Rev. Plant Biol.* *53*, 329–355.
- Osterlund, M.T., Hardtke, C.S., Wei, N., and Deng, X.W. (2000). Targeted destabilization of HY5 during light-regulated development of Arabidopsis. *Nature* *405*, 462–466.
- Pickart, C.M. (2001). Mechanisms underlying ubiquitination. *Annu. Rev. Biochem.* *70*, 503–533.
- Ryu, J.S., Kim, J.I., Kunkel, T., Kim, B.C., Cho, D.S., Hong, S.H., Kim, S.H., Fernandez, A.P., Kim, Y., Alonso, J.M., et al. (2005). Phytochrome-specific type 5 phosphatase controls light signal flux by enhancing phytochrome stability and affinity for a signal transducer. *Cell* *120*, 395–406.
- Saijo, Y., Sullivan, J.A., Wang, H.Y., Yang, J.P., Shen, Y.P., Rubio, V., Ma, L.G., Hoecker, U., and Deng, X.W. (2003). The COP1-SPA1 interaction defines a critical step in phytochrome A-mediated regulation of HY5 activity. *Genes Dev.* *17*, 2642–2647.
- Seo, H.S., Watanabe, E., Tokutomi, S., Nagatani, A., and Chua, N.H. (2004). Photoreceptor ubiquitination by COP1 E3 ligase desensitizes phytochrome A signaling. *Genes Dev.* *18*, 617–622.
- Seo, H.S., Yang, J.Y., Ishikawa, M., Bolle, C., Ballesteros, M.L., and Chua, N.H. (2003). LAF1 ubiquitination by COP1 controls photomorphogenesis and is stimulated by SPA1. *Nature* *423*, 995–999.
- Shen, Y.P., Feng, S.H., Ma, L.G., Lin, R.C., Qu, L.J., Chen, Z.L., Wang, H.Y., and Deng, X.W. (2005). Arabidopsis FHY1 protein stability is regulated by light via phytochrome A and 26S proteasome. *Plant Physiol.* *139*, 1234–1243.
- Shinomura, T., Uchida, K., and Furuya, M. (2000). Elementary processes of photoperception by phytochrome A for a high-irradiance response of hypocotyl elongation in Arabidopsis. *Plant Physiol.* *122*, 147–156.
- Wang, H.Y., and Deng, X.W. (2002). Arabidopsis FHY3 defines a key phytochrome A signaling component directly interacting with its homologous partner FAR1. *EMBO J.* *21*, 1339–1349.
- Wang, H.Y., Ma, L.G., Habashi, J., Li, J.M., Zhao, H.Y., and Deng, X.W. (2002). Analysis of far-red light-regulated genome expression profiles of phytochrome A pathway mutants in Arabidopsis. *Plant J.* *32*, 723–733.
- Yang, J.P., Lin, R.C., James, S., Hoecker, U., Liu, B.L., Xu, L., Deng, X.W., and Wang, H.Y. (2005). Light regulates COP1-mediated degradation of HFR1, a transcription factor essential for light signaling in Arabidopsis. *Plant Cell* *17*, 804–821.
- Yeh, K.C., and Lagarias, J.C. (1998). Eukaryotic phytochromes: Light-regulated serine/threonine protein kinases with histidine kinase ancestry. *Proc. Natl. Acad. Sci. USA* *95*, 13976–13981.
- Zhou, Q., Hare, D.P., Yang, W.S., Zeidler, M., and Chua, N.-H. (2005). FHL is required for full phytochrome A signaling and shares overlapping functions with FHY1. *Plant J.* *43*, 356–370.

Supplemental Data

Arabidopsis COP1/SPA1 Complex and Differential Phosphorylation of Phytochrome A in Balancing Signal Propagation and Attenuation

Yusuke Saijo, Danmeng Zhu, Jigang Li, Vicente Rubio, Zhenzhen Zhou, Yunping Shen, Ute Hoecker, Haiyang Wang, and Xing Wang Deng

Supplemental Experimental Procedures

Plant materials and growth conditions

The wild-type plants used were of the Columbia (Col) ecotype unless otherwise stated. The *cop1*, *spa1-3*, *spa1-3 spa2-1 spa3-1*, and *spa1-3 spa2-1 spa4-1* mutants used have been described (Hoecker et al., 1998; Laubinger et al., 2004; McNellis et al., 1996). The phyA-signaling mutants used were *phyA-101* (ecotype RLD, Figure 2), *phyA-211* (ecotype Col, Figure 3), *phyA-1* (ecotype L.er, Figure S7), *fhy3-1*, *fhy3-1 far1-2*, and *fhy1-1* (Desnos et al., 2001; Hoecker et al., 1998; Osterlund et al., 2000; Reed et al., 1994; Wang and Deng, 2002). The phyA-overexpression line (ecotype L.er) has been described (Osterlund et al., 2000). The oat phyA-expression lines have been described (Kim et al., 2004). MG132 and cycloheximide treatments were performed as previously described (Osterlund et al., 2000; Saijo et al., 2003).

TSC purification

We followed basic procedures as previously described (Rubio et al., 2005) with the following modifications. Protein extraction for IgG-Sepharose (Amersham Biosciences) precipitation was performed with lysis buffer A (Saijo et al., 2003) containing 200 mM NaCl, 0.5 mM DTT and 20 μ M MG132 (buffer B). For co-precipitation of TAPSPA1 with phyA (Figure S1C), acid-eluates of the IgG Sepharose precipitates in the lysis buffer containing 150 mM NaCl were recovered. Buffer C (50 mM Tris pH 7.5, 150 mM NaCl, 10% glycerol, 1 mM DTT, and 0.1% Tween20) was used in the 3C-Protease (Amersham Biosciences) cleavage reactions. Supernatants recovered were subjected to gel filtration chromatography (Saijo et al., 2003). The fractions enriched with both proteins (fractions number 6-11 in Figure S1A) were concentrated with Microcon YM-50 (Millipore) according to the manufacturer's instruction, and used for *in vitro* E3 assays in Figure 1C. For mass spectrometry and E3 assays in Figure 1B, gel filtration chromatography of the 3C-Protease cleaved products was carried out in buffer D (phosphate buffer saline pH 7.4, 200 mM NaCl, 10% glycerol and 0.1% Tween 20). There were no detectable changes in the fractionation of TSC in both buffer conditions. The fractions number 6-11 enriched with both proteins were collected and subjected to His₆-tag

purification with Ni-NTA resin (Qiagen) in buffer E (phosphate buffer saline pH7.4, 250 mM NaCl, 10% glycerol and 10 mM imidazole). After extensive washing with buffer E, elution was performed with buffer F (phosphate buffer saline pH7.4, 140 mM NaCl, 150 mM imidazole). For mass spectrometry analysis, proteins were recovered from the eluates by STRATARESIN (Stratagene) and then separated on an 8~12% SDS-polyacrylamide gel electrophoresis (PAGE) gradation gel. Protein bands were sliced out of the gel after staining with SYPRO Ruby Stain (Invitrogen). For E3 assays in Figure 1B, the eluates from Ni-Sepharose concentrated with Microcon YM-50 and dialyzed were used.

In vitro E3 assays

Ubiquitination reaction mixtures contained 40 mM Tris-HCl pH 7.5, 50 mM NaCl, 20 μ M ZnCl₂, 5 mM MgCl₂, 2 mM ATP, 2 mM DTT, 2% glycerol, 2.5 μ M ubiquitin-Aldehyde (Boston Biochem), 75 ng rabbit E1 (Boston Biochem), 75 ng each of human UbcH5b (Boston Biochem) and rice His₆-Rad6 (Yamamoto et al., 2004) as the E2, and 10 μ g of unlabelled ubiquitin (in Figure 1B) or 10 μ g of Flag-ubiquitin and 7 μ g of unlabelled ubiquitin (both from Boston Biochem) (in Figure 1C) in a total volume of 50 μ l. Over 8 μ g GST was added together with or without 500 ng GSTphyA as the substrate. In addition, approximately 100 ng

of purified Arabidopsis TSC (Ni-Sepharose eluates for Figure 1B and Superose 6 fractions number 6-11 at an analytical scale for Figure 1C), or the corresponding TAPGFP preparation as a negative control, was pre-incubated on ice for 30 min in a buffer containing 50 mM Tris-Cl pH 7.5, 150 mM NaCl, 10% glycerol, 0.1% Tween20, 0.5 mM DTT and 100 M ZnCl₂, and then added to the reaction mixture. After incubation at 30 degrees Celsius for over 2 h, reactions were terminated by the addition of SDS sample buffer. For IP, reactions were boiled in TBST (50 mM Tris pH 7.5, 150 mM NaCl, 0.1% Tween20) with 1% SDS for 5 min, and then diluted to 0.1% SDS by TBST. IP was performed with anti-GST antibody (Amersham) at room temperature essentially as described above, with the aim of specifically precipitating GSTphyA. Ubiquitinated products and immunoprecipitates were separated on 7% SDS-PAGE gels, and then detected by immunoblotting with anti-GST or anti-Flag antibody M2 (Sigma).

Antibodies

The polyclonal antibodies against COP1, CSN3, CSN6, Rpt5, and Cul3, and the monoclonal phyA and myc antibodies were prepared previously (Figueroa et al., 2005; McNellis et al., 1996; Saijo et al., 2003; Sharrock and Clack, 2002). We generated rabbit polyclonal SPA1

and FHY3 antibodies as described previously (Osterlund et al., 2000), using a bacterially expressed GST fusion protein of the FHY3 C-terminal portion (amino acid residues 541-839) and a His₆-tag fusion protein of the SPA1 N-terminal portion (amino acid residues 1-273) as antigens.

Immunoblot analysis and immunoprecipitation (IP)

For immunoblot analysis, gel filtration chromatography, and IP, we used a buffer containing 50 mM Tris at pH 7.5, 200 mM NaCl, 1 mM EDTA, 10 mM NaF, 25 mM beta-glycerophosphate, 2 mM sodium orthovanadate, 10% (w/v) glycerol, 0.1 mM Tween 20, 0.5 mM DTT, 1 mM PMSF, and 1 x complete protease inhibitor cocktail (Roche) for lysis and subsequent procedures unless otherwise stated. For IP, the extracts were pre-incubated with Protein-A Sepharose (Sigma), and then recovered supernatants were incubated with the indicated antibodies at 4 degree Celsius for 2 h followed by further incubation for 1 h with Protein-A Sepharose.

Phosphatase treatment

Protein phosphatase treatment was performed with calf intestinal alkaline phosphatase (CIP;

New England Biolabs) according to the manufacturer's instructions. For the assay in Figure 3F, 1x complete protease inhibitor cocktail (Roche), 1 mM PMSF and 25 μ M MG132 were added to the buffer used for protein extraction and subsequent CIP incubation.

Nuclear fractionation

Nuclear fractionation was performed essentially as previously described (Shen et al., 2007) with the following modifications. The same amounts of fresh weight of different seedling tissue samples were homogenized in a modified Honda buffer [Honda et al., 1966; 2.5% Ficoll 400, 5% dextran T40, 0.4 M sucrose, 25 mM Tris-HCl pH 7.5, 10 mM MgCl₂, 10 mM NaF, 25 mM β -glycerophosphate, 2 mM sodium orthovanadate, 1 mM DTT, 1 mM PMSF, and 1 x complete protease inhibitor cocktail (Roche)] using a mortar and pestle, and then filtered through a 62 μ m pore-size nylon mesh. After Triton X-100 addition to a final concentration of 0.5%, the homogenate was incubated on ice for 15 min and centrifuged at 1,500 g for 5 min. The supernatant fraction was saved (soluble, nuclear-depleted fraction) and the pellet was subsequently reprocessed to further purify the nuclear fraction as previously described (Shen et al., 2007). An approximately 12-fold quantity (in protein content) of the nuclear fraction compared to the nuclear-depleted soluble fraction on a per-tissue amount

basis was subjected to immunoblot analysis. Anti-histone H3 antibodies (Abcam) were used as a nuclear fraction marker, and anti-phosphoenolpyruvate carboxylase (PEPC) (Rockland Immunochemicals) and anti-HSP90 antibodies (Santa Cruz Biotechnology) were used as soluble fraction markers.

Supplementary References

Desnos, T., Puente, P., Whitelam, G. C., and Harberd, N. P. (2001). FHY1: a phytochrome A-specific signal transducer. *Genes & Development* *15*, 2980-2990.

Figuroa, P., Gusmaroli, G., Serino, G., Habashi, J., Ma, L. G., Shen, Y. P., Feng, S. H., Bostick, M., Callis, J., Hellmann, H., and Deng, X. W. (2005). Arabidopsis has two redundant Cullin3 proteins that are essential for embryo development and that interact with RBX1 and BTB proteins to form multisubunit E3 ubiquitin ligase complexes in vivo. *Plant Cell* *17*, 1180-1195.

Hoecker, U., Xu, Y., and Quail, P. H. (1998). SPA1: A new genetic locus involved in phytochrome A - Specific signal transduction. *Plant Cell* *10*, 19-33.

Honda, S. I., Honglada, T., and Laties, G. G. (1966). A new isolation medium for plant organelles. *J. Exp. Botany* *17*, 460-472.

Kim, J., Shen, Y., Han, Y. J., Park, J. E., Kirchenbauer, D., Soh, M. S., Nagy, F., Schafer, E., and Song, P. S. (2004). Phytochrome phosphorylation modulates light signaling by influencing the protein-protein interaction. *Plant Cell* *16*, 2629-2640.

Laubinger, S., Fittinghoff, K., and Hoecker, U. (2004). The SPA quartet: A family of WD-repeat proteins with a central role in suppression of photomorphogenesis in arabidopsis.

Plant Cell *16*, 2293-2306.

McNellis, T. W., Torii, K. U., and Deng, X. W. (1996). Expression of an N-terminal fragment of COP1 confers a dominant-negative effect on light-regulated seedling development in Arabidopsis. Plant Cell *8*, 1491-1503.

McNellis, T. W., Vonarnim, A. G., and Deng, X. W. (1994). Overexpression of Arabidopsis Cop1 Results in Partial Suppression of Light-Mediated Development - Evidence for a Light-Inactivable Repressor of Photomorphogenesis. Plant Cell *6*, 1391-1400.

Osterlund, M. T., Hardtke, C. S., Wei, N., and Deng, X. W. (2000). Targeted destabilization of HY5 during light-regulated development of Arabidopsis. Nature *405*, 462-466.

Reed, J. W., Nagatani, A., Elich, T. D., Fagan, M., and Chory, J. (1994). Phytochrome-a and Phytochrome-B Have Overlapping but Distinct Functions in Arabidopsis Development. Plant Physiology *104*, 1139-1149.

Rubio, V., Shen, Y. P., Saijo, Y., Liu, Y. L., Gusmaroli, G., Dinesh-Kumar, S. P., and Deng, X. W. (2005). An alternative tandem affinity purification strategy applied to Arabidopsis protein complex isolation. Plant J. *41*, 767-778.

Saijo, Y., Sullivan, J. A., Wang, H. Y., Yang, J. P., Shen, Y. P., Rubio, V., Ma, L. G., Hoecker, U., and Deng, X. W. (2003). The COP1-SPA1 interaction defines a critical step in

phytochrome A-mediated regulation of HY5 activity. *Genes & Development* *17*, 2642-2647.

Sharrock, R. A., and Clack, T. (2002). Patterns of expression and normalized levels of the five *Arabidopsis* phytochromes. *Plant Physiology* *130*, 442-456.

Shen, Q. H., Saijo, Y., Mauch, S., Biskup, C., Bieri, S., Keller, B., Seki, H., Ulker, B., Somssich, I. E., and Schulze-Lefert, P. (2007). Nuclear activity of MLA immune receptors links isolate-specific and basal disease-resistance responses. *Science* *315*, 1098-1103.

Shen, Y. P., Feng, S. H., Ma, L. G., Lin, R. C., Qu, L. J., Chen, Z. L., Wang, H. Y., and Deng, X. W. (2005). *Arabidopsis* FHY1 protein stability is regulated by light via phytochrome a and 26S proteasome. *Plant Physiology* *139*, 1234-1243.

Wang, H. Y., and Deng, X. W. (2002). *Arabidopsis* FHY3 defines a key phytochrome A signaling component directly interacting with its homologous partner FAR1. *Embo Journal* *21*, 1339-1349.

Yamamoto, T., Mori, Y., Ishibashi, T., Uchiyama, Y., Sakaguchi, N., Furukawa, T., Hashimoto, J., Kimura, S., and Sakaguchi, K. (2004). Characterization of Rad6 from a higher plant, rice (*Oryza sativa* L.) and its interaction with Sgt1, a subunit of the SCF ubiquitin ligase complex. *Biochemical and Biophysical Research Communications* *314*, 434-439.

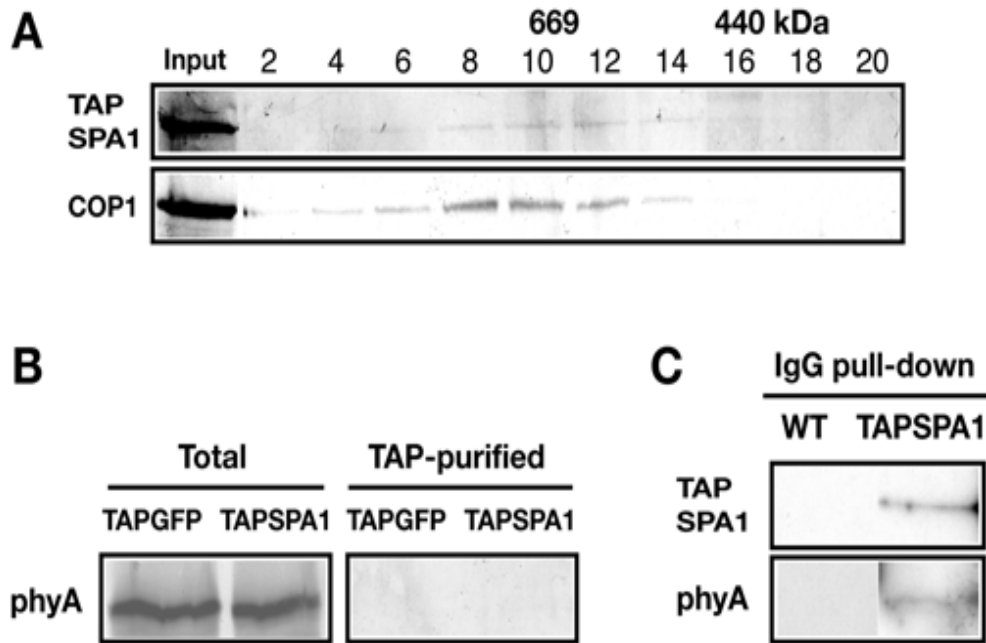


Figure S1. Characterization of the TAPSPA1-COP1 complex (TSC)

(A) Gel filtration profiles of TAPSPA1 and COP1 in the purified TSC. The indicated fractions eluted from the Superose 6 column were subjected to immunoblot analysis with anti-myc (for TAPSPA1) and COP1 antibodies. Molecular weight is indicated above. The fractions from 6 to 11 were collected and used for subsequent purification and ubiquitination assays. (B) Immunoblot analysis for phyA in the TAP-purified proteins and total lysates. (C) TAPSPA1 co-precipitates with phyA from dark-grown seedlings. IgG-precipitation (only the first step of our TAP procedures) was performed in less stringent conditions (in a buffer containing 150 mM NaCl) and then subjected to immunoblotting with myc (TAPSPA1) and phyA antibodies. TAPSPA1, a TAPSPA1 transgenic line in the *spa1-3* background (Saijo et al., 2003); WT,

wild type RLD.

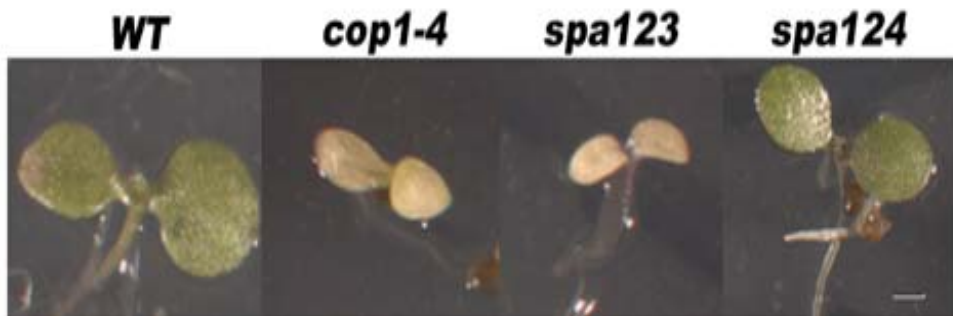


Figure S2. The phyA-dependent FR block of greening is more pronounced in *spa1 spa2 spa3 (spa123)* compared to *spa1 spa2 spa4 (spa124)* triple mutants

Five-day-old FRc-grown seedlings were transferred to Rc for 2 days. Bar = 1 mm.

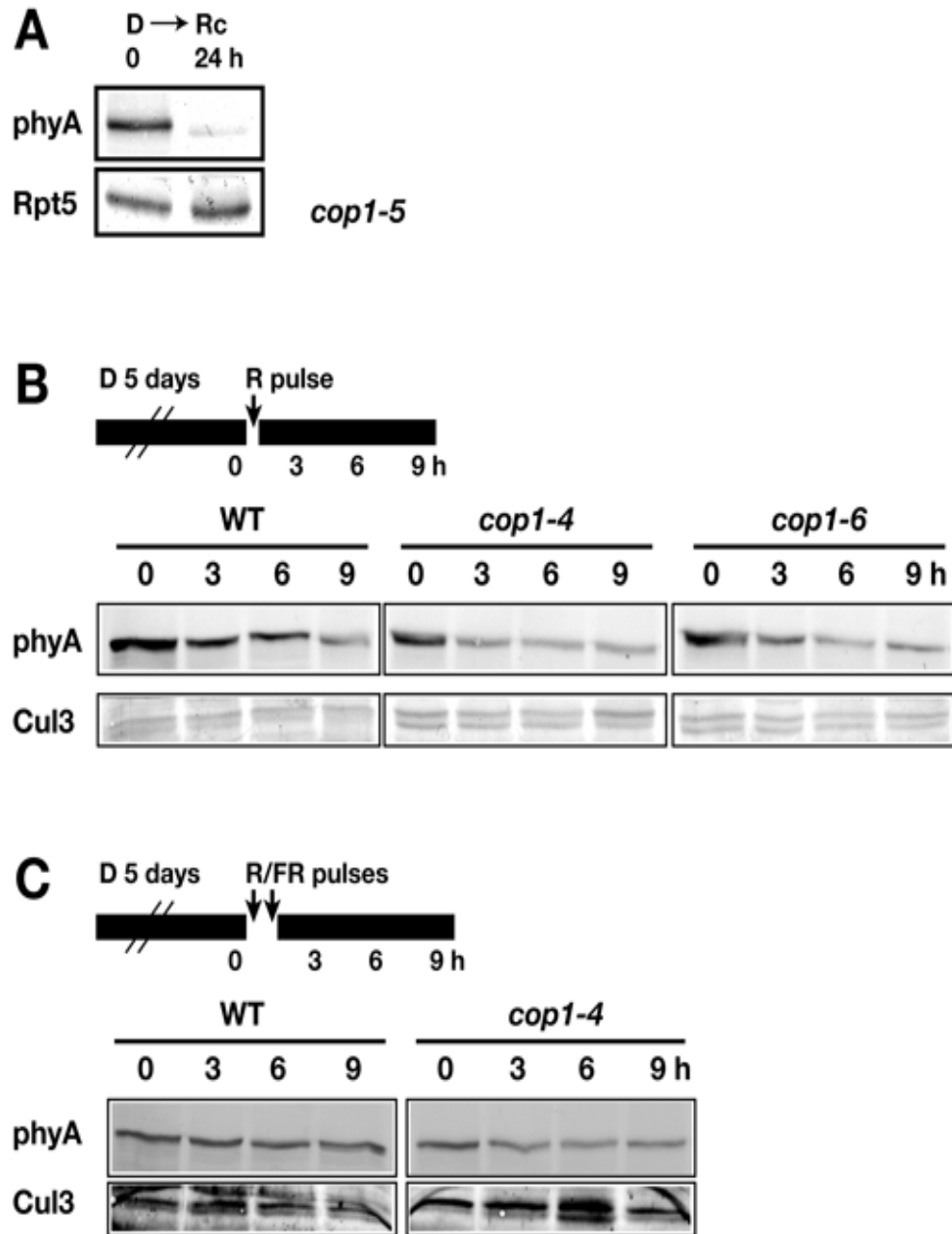


Figure S3. COP1-independent pathway for light-induced phyA degradation

(A) Five-day-old dark-grown *cop1-5* null mutant seedlings were exposed to Rc for 24 h and then subjected to immunoblot analysis with the indicated antibodies.

(B and C) Five-day-old dark-grown seedlings were irradiated with 5-min R pulse (B) or

5-min R pulse followed by 5-min FR pulse (C), and then kept under darkness for the indicated times. phyA abundance was monitored by immunoblot analysis. The Cul3 blots were shown as a loading control.

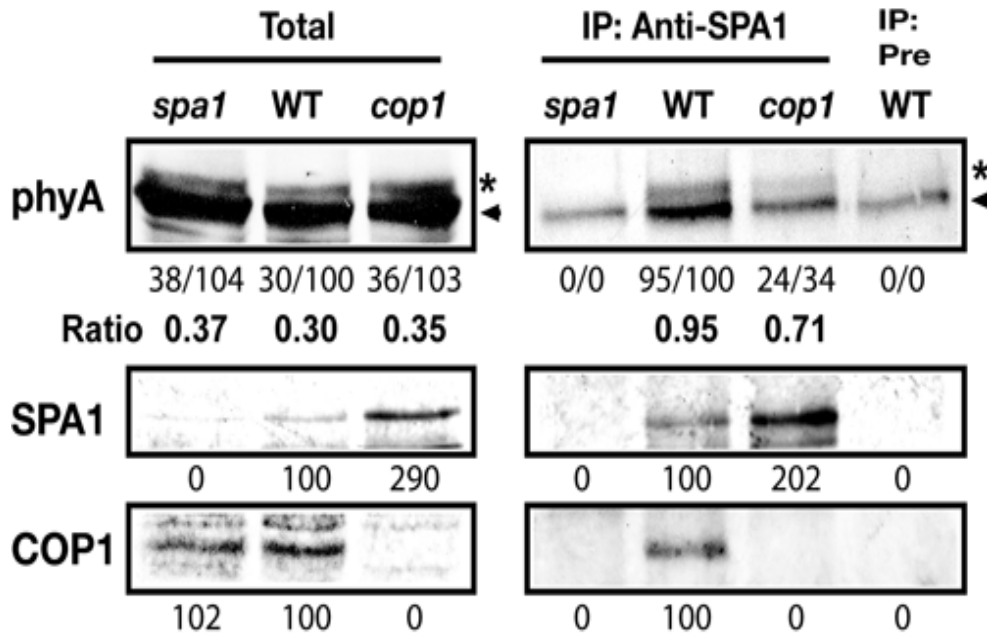


Figure S4. COP1 and SPA1 act together to recruit phyA

FRC-grown wild-type (WT), *spa1-3* (*spa1*) and *cop1-4* (*cop1*) seedlings were subjected to IP analysis with anti-SPA1 antibodies. The asterisk and arrowhead respectively represent phosphorylated and underphosphorylated phyA. Relative band intensities normalized for each panel and the ratio of phosphorylated to underphosphorylated phyA are shown. A truncated COP1-4 protein (containing amino acid residues 1-282), which lacks the WD40 domain

responsible for direct phyA interaction (Seo et al., 2004), is expressed in *cop1-4* (McNellis et al., 1996). We note a weak but positive co-IP between SPA1 and phyA in *cop1-4*. A weak SPA1-phyA association may occur through the WD40 domain of SPA1. As the mutant COP1-4 protein can still interact with SPA1 via the residual SPA1-binding coiled-coil domain (Saijo et al., 2003), the interaction between COP1-4 and SPA1 may retain partial function of the COP1/SPA1 complex.

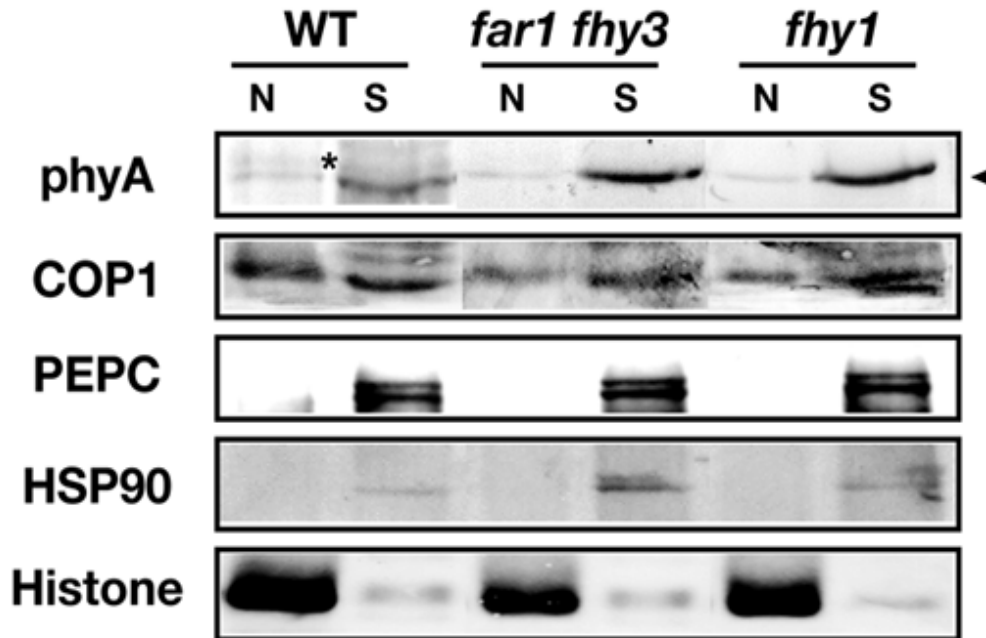


Figure S5. Reduced Nuclear accumulation of phyA in the *fhy3 far1* and *fhy1* mutants

Purified nuclear (N) and nuclei-depleted soluble (S) fractions were prepared from 5-day-old FRC-grown wild type, *fhy3 far1* and *fhy1* mutant seedlings. The proteins were subjected to

immunoblot analyses. Histone H3 (Histone) and cytosolic HSP90 and phosphoenolpyruvate carboxylase (PEPC) were used as fraction markers. The asterisk and arrowhead respectively represent cap-phyA and underphosphorylated phyA.

At phyA	MGGSRFTQSSSEGRSRHSARI IAQTTVDAKLHADFEESGSSFDYSTSVKVTGPPVENQPPRSDEKVTITTLHEHQKGLIQPFQCLLALD	90
oat phyA	MSSSRFA [*] SSSSRNHQSSQARVLAQTTIDAELNAETESGDSFDYSKLVEAQDGPFPVQQRSEKVI A-TLQHIQKGLIQTFQCLLALD	89
	** * * * *	
At phyA	EKTFKVIATSENAPELLTMASHAVPSVGERFVLGIGTDIRSLFTAPASALQKALGFDVLLNPIIVHCRTSAKFFTAIHRVGTGSI I	180
oat phyA	EKSPNVIAFSENAPEMLTTVSHAVPSVDDFFRLGIGTRVSLFSDQGATALEKALGFADVLLNPIIVQCKTSGKFFTAIVHRATGCLLV	179
	** * * * *	
At phyA	DFEPVKPTEFPATAAGALQSTKLAAKAITRLQSLFSGSHERLCDTMSVQEVFELGTDRVMAKPFREDDHGEVSEVTKFGLPFLGLHYP	270
oat phyA	DFEPVKPTEFPATAAGALQSTKLAAKAISKIQSLFSGSMEVLCNTVVKVDFDLGTDRVMAKPFREDDHGEVSEITKFGLEPFLGLHYP	269
	** * * * *	
At phyA	ATDIPQAARFLPMSGKVMIVDCBAKHARVLQDEKLSFDLTLGCGSTLRAPHSCHLQTHASBDSIASLVMAVVVNEEDGEGDAFDATT-QP	359
oat phyA	ATDIPQAARFLPMSGKVMICDCRARSIKVIEAEALFPDISLGGALRAHPSCHLQTHMBDSIASLVMAVVVNEEDDEAESEQFAQQ	359
	** * * * *	
At phyA	QKRRKLNGLVVCNTTTPRVPFFFLRYACEFLAQVFATVHNKEVELDNQVVEENILRTQTLLCDMLARDA-PLGIVSQSPNIMDLVKCDGA	448
oat phyA	QKRRKLNGLVCHHESPRVFPFLRYACEFLAQVFVAVHVRFELEKQLREKNILRMQTMLSMDLFRASPLTIVSGTNNIMDLVKCDGA	449
	** * * * *	
At phyA	ALLTKDKIKLQTTSEPHLQEIASWLCETHMDSTGLSTDSLHDAGFFRALSLGDSVCGMAAVRISKDMIWFPRSHTAGVVRWGGAKHD	538
oat phyA	ALLYGGVWRKLNAPTESQIHDIAPWLSVWRDSTGLSTDSLHDAGYFGAALGDMICGMVAKIHSKDLFPFRSHTAAEIRWGGAKND	539
	** * * * *	
At phyA	PDSDRDARRMHPRSSFKAFLEVVVKTRSLPKDYEMDAIHSLLQLLNAPKDSSETDVTNKVIYSKLNDLKIDGIQLEAVTSEMVRLIET	628
oat phyA	PSDMDSRMHPRLSFKAFLEVVVKSLPMSDYEMDAIHSLLQLLNAPKDSSETDVTNKVIYSKLNDLKIDGIQLEAVTSEMVRIMET	628
	** * * * *	
At phyA	ATVPII AVDSGLVGNWHTKIAELTGLSVDEAIGKHFLTLVDESSVEIVKRGLENALGTEEQVQVFEIKRHLRADAGPISLVVWACAS	718
oat phyA	ATVPII AVDGNGLVGNWQKAAELTGLRVDDAIGRHILTLVDESSVPPVQRRLYLALQKKEEKEVFEVKTNGPKRDDGPPVILVWACAS	718
	** * * * *	
At phyA	RDLHEHVGVVCFVANDLTGQRTVMDKFTRIEGDYKAI IQNPHLI PPIFGTDFGWCETERNPAMSKLTGLKREVIDMQLLGEVFGTQKS	808
oat phyA	RDLHEHVGVVCFVAGMTVHKLVMDKFTRVGQYKAI IHNPHLI PPIFGADEFGWCSEWNAAMTKLTGNRDEVLDMQLLGEVFDSSNA	808
	** * * * *	
At phyA	CCRLQKQAEFVNLGIVLNAVTSQDFEKVSFAFFTRGGKYVECLLCSKLDREGVVTGVFCFLQLASHELQALHVQRLAERTAVKRLK	898
oat phyA	SCPLKQKDAFVSLCVLINSALAGEETEKAFFGFFDRSGKYIECLLSANRKEHEGGLITGVFCFIHVASHELQALVQQASEQTSKRLK	898
	** * * * *	
At phyA	ALAYIKRQIRNPLSGIMFTRFMIEGTGLGPEQRRI LQTSALCQKQKLSKILDSDLESII EG--CLDLEMKEFTLNEVLTASTSQVMKSN	986
oat phyA	AFSTYMRHAINNPLSGMLYSRKALKNTDLNKEQKQI NVGDNCHHQINKILADLQDSITEKSSCLDLEMKEFTLNEVLTASTSQVMKSN	988
	** * * * *	
At phyA	GKSVRITNETGKEVMSDTLYGDSIRLQQVLADPHLMAVHFTPSGGQLTVSASLRKDQLGRSVHLANLEIRLTHTGAGIPEFLINQMGTE	1076
oat phyA	GKGI RISCHELPERFMQSVYGDGVRLLQQLSDFLFISVKFSPVGGVVEISSKLTNNSIGENLRLIDLELRIRKQGLGVPAELMAQMFEE	1078
	** * * * *	
At phyA	EDV-SEEGLSLMVSRKLVKLMNGDVQYLRQAGKSSFIITAE LAANK---	1122
oat phyA	NKQSEEGLSLIVSRNLRLMNGDVRHLREAGVSTFIITAE LASAPTAMQ	1129
	** * * * *	

Figure S6. Amino acid sequence alignment of Arabidopsis and oat phyA

Arabidopsis (At) and oat phyA amino acid sequences are aligned. Identical residues are indicated by asterisks. The Ser residues on oat phyA identified as *in vivo* phosphorylation

sites are highlighted in red. The number of amino acid residues is shown on the right.

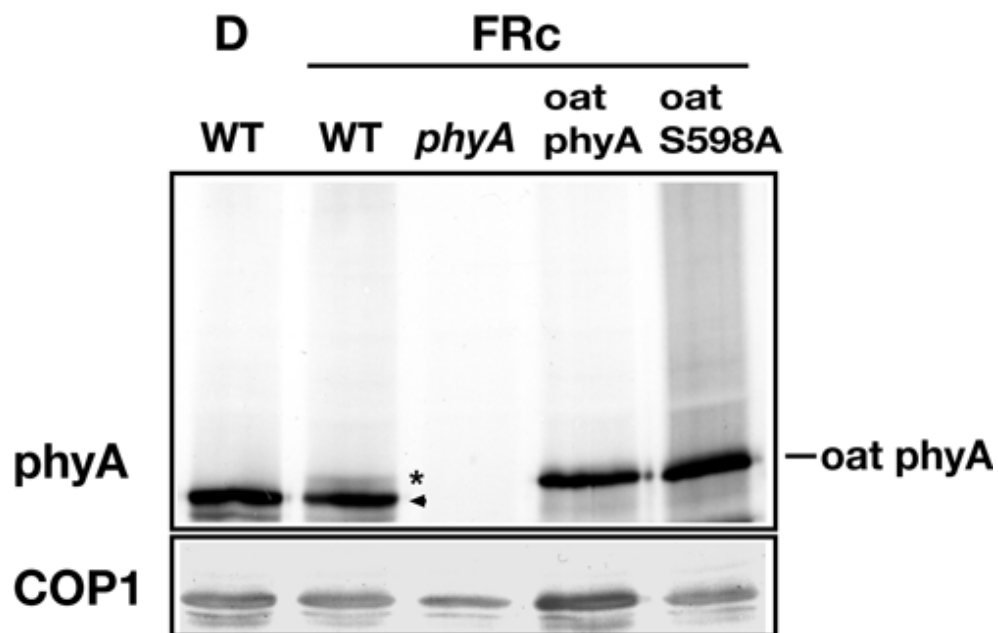


Figure S7. Immunoblot analysis of Arabidopsis seedlings expressing oat phyA

Five-day-old dark (D)- and FRc-grown Arabidopsis seedlings were subjected to immunoblot analysis with anti-phyA and anti-COP1 antibodies. The wild type (WT) ecotype used was *Ler*. Transgenic Arabidopsis seedlings expressing oat wild-type phyA or a point-substituted phyA form at the identified phosphorylation site Ser598 (S598A) in the *phyA-1* background were used. The positions of cap-phyA and underphosphorylated phyA are indicated by the asterisk and arrowhead, respectively.

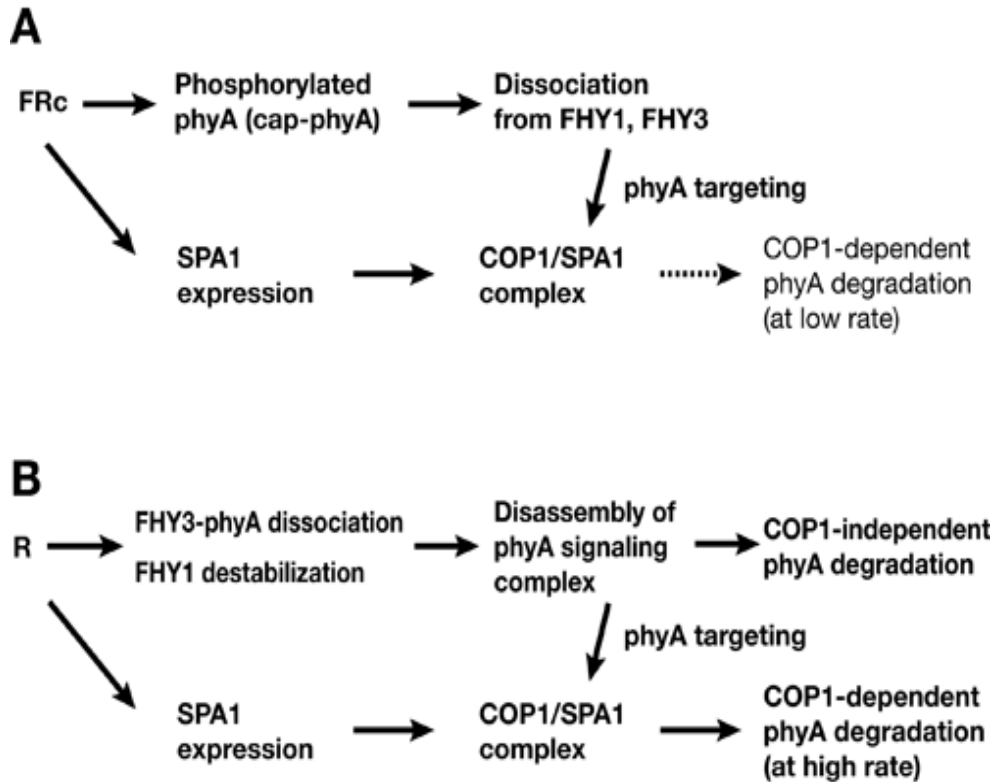


Figure S8. Model for desensitization of phyA signaling

(A) Under FRc, phyA signaling activation by prolonged FRc is accompanied with production of a cap-phyA pool and an elevation in SPA1 abundance. phyA phosphorylation lowers its affinity to FHY1 and FHY3/FAR1, and then leads to its dissociation from these signaling intermediates that predominantly associate with underphosphorylated phyA. As a consequence, cap-phyA preferentially associates with the COP1/SPA1 complex that is increased by high SPA1 accumulation. FHY3, FAR1 and FHY1 likely prevent the recruitment of phyA (mainly in Pr form under FRc) to the COP1/SPA1 complex. Notably, the COP1/SPA1 complex recognition of cap-phyA is not sufficient to trigger high-rate phyA

degradation.

(B) Upon R irradiation, phyA-Pfr (PfrA) dissociation from the FHY3-containing signaling complex and FHY1 destabilization stimulate targeting of phyA, despite its phosphorylation status, for degradation via both COP1-dependent and independent pathways. R-induced increase in the COP1/SPA1 complex formation following SPA1 up-regulation should enhance the activity of a COP1-dependent pathway.